Spin Electronics

Spin-Transfer Torque Switching Above Ambient Temperature

Hui Zhao[1*], Pedram Khalili Amiri[2**], Yisong Zhang[1], Andrew Lyle[1*], Jordan A. Katine[3***], Juergen Langer[4], Hongwen Jiang[5], Kang L. Wang[2†], Ilya N. Krivorotov[6**], and Jian-Ping Wang[1**]

[1] *Department of Electrical and Computer Engineering, University of Minnesota, Minneapolis, MN 55455, USA*
[2] *Department of Electrical Engineering, University of California, Los Angeles, CA 90095, USA*
[3] *Hitachi Global Storage Technologies, San Jose, CA 95135, USA*
[4] *Singulus Technologies, 63796 Kahl, Germany*
[5] *Department of Physics and Astronomy, University of California, Los Angeles, CA 90095, USA*
[6] *Department of Physics and Astronomy, University of California, Irvine, CA 92697, USA*
[*] *Student Member, IEEE*
[**] *Member, IEEE*
[***] *Senior Member, IEEE*
[†] *Fellow, IEEE*

Received 16 March 2012, revised 6 April 2012, accepted 11 April 2012, published 24 May 2012.

Abstract—We report the temperature dependences of tunneling magnetoresistance ratio, coercivity, thermal stability, and switching current distribution of magnetic tunnel junctions (MTJs) in the temperature range 25–80 °C, the most probable working environment for spin-transfer torque random access memory (STT-RAM). Two distinct temperature dependence of the switching current density are apparent due to two switching mechanisms: a switching current density decrease with increasing temperature in the long-pulse (>1 μs) regime, a result of thermally activated switching, but no decrease in the short-pulse (<10 ns) regime, as a result of precessional switching. In the temperature range studied, the switching current density variation is less sensitive to environmental temperature than it is to switching time. Thus, switching time is the more important factor to consider in STT-RAM design.

Index Terms—Spin electronics, magnetic tunnel junction (MTJ), spin-transfer torque switching, spin-transfer torque random access memory (STT-RAM).

I. INTRODUCTION

A new nonvolatile memory spin-transfer torque random access memory (STT-RAM), based on magnetic tunnel junctions (MTJ), is currently under fast development [Katine 2008, Chen 2010, Min 2010, Kawahara 2011]. Current-induced spin-transfer torque (STT) switching is used for the STT-RAM writing operation due to its advantages in energy efficiency and circuit scalability [Slonczewski 1996, Berger 1996]. The MTJ memory cell and its STT switching properties have been studied intensively for STT-RAM application [Higo 2005, Meng 2006, Wang 2009, Heindl 2011, Seki 2011, Zhao 2011]. Meanwhile, it is crucial to understand the temperature-dependent performance of MTJ cells and STT switching for real STT-RAM applications, since the STT-RAM often has to work in a heated environment above room temperature (RT), especially when it is used as an embedded memory. Until now, most of the previous reports were performed at RT or low temperature. Myers et al. [2002] studied the switching current dependence at low temperature from 180 K to 220 K in nanomagnets with a pseudospin-valve stack structure. Krivorotov et al. [2004] reported the temperature dependence of the dwell time for the resistance fluctuation with spin-polarized current injection from 4.2 to 295 K in a similar structure. To the best our knowledge, no experimental work on MTJ-based STT switching performance has been reported at the potential working temperature for STT-RAM above RT.

In this letter, we investigate the STT switching performance of MTJs above the RT (25 °C–80 °C). The particular temperature range is chosen to imitate the real working environment of STT-RAM application. The tunneling magnetoresistance (TMR) ratio, coercivity, thermal stability, and switching current density are studied. In particular, we report the mean and distribution values of STT switching current density for pulse widths ranging from 1 ns to 0.1 s at various temperatures. The effects of the environmental temperature on the distribution of the switching current density will be experimentally analyzed and correlated with different switching mechanisms.

II. EXPERIMENT

The samples studied here have a standard in-plane stack structure, MgO MTJ structure of (bottom electrode)/PtMn (15 nm)/$Co_{70}Fe_{30}$ (2.5 nm)/Ru (0.85 nm)/$Co_{40}Fe_{40}B_{20}$ (2.4 nm)/MgO (0.83 nm)/$Co_{20}Fe_{60}B_{20}$ (2.0 nm)/(top electrode). They were deposited using a Singulus TIMARIS sputtering system followed by a post annealing process at 300 °C under 1 T magnetic field for 2 h. The thin-film stack was patterned into elliptical nanopillars with various sizes and aspect ratios. The results shown in this letter were measured in MTJs with two lateral dimensions, 50 nm $\times$ 110 nm and 50 nm $\times$ 170 nm.

The whole sample chip was heated by a film resistance heater (maximum power density 10 W/in^2) attached on the back side of the chip. Meanwhile, we also attached a reference chip on the same film resistance heater and monitored its temperature by a thermal couple during the heating process. Since the reference chip was chosen to have the same size and material as the

Corresponding author: J.-P. Wang (jpwang@umn.edu).
Digital Object Identifier: 10.1109/LMAG.2012.2195775

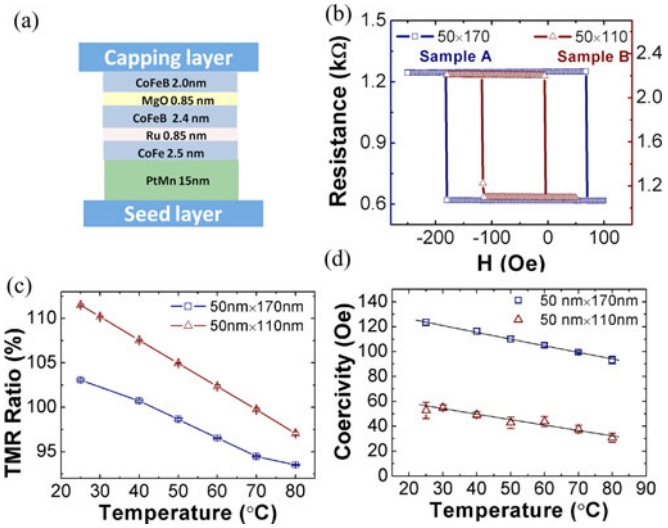

Fig. 1. (a) Schematic of an MTJ device stack structure. (b) Resistance versus magnetic field loop of Sample A (50 nm × 170 nm) and Sample B (50 nm × 110 nm). (c) and (d) TMR ratio and coercivity dependence on temperature of the two samples.

sample chip, the temperature of the two chips should be identical. The heating process was controlled by the proportional-integral-derivative feedback mechanism with less than 1 °C temperature fluctuation.

The temperature dependence of TMR ratio and coercivity was tested from 25 °C to 80 °C. The STT switching cumulative distribution function (CDF) from antiparallel state to parallel state was characterized in a broad time range from 1 ns to 0.1 s and at three environmental temperatures: 25 °C, 50 °C, and 75 °C. The switching CDF was collected by the switching probability measurement in a manner similar to previous work [Zhao 2011] under zero effective bias field. Hundred trials were used in the measurement for each probability point. Switching pulses from 10 ns to 0.1 s were generated by a H-P 8110 A pulse generator with 2 ns rise and fall time. Shorter than 10 ns switching pulses were generated by a Picosecond 10070 A pulse generator with a rise and fall time of 65 and 85 ps, respectively.

III. RESULTS AND DISCUSSION

The resistance versus magnetic field loops of MTJ samples (Sample A: 50 nm × 170 nm and Sample B: 50 nm × 110 nm) at RT are given in Fig. 1(b). With the increase in aspect ratio from 2.2 to 3.4, the free layer coercivity doubles from 53 Oe to 123 Oe. Due to the coupling with the pinned layer, a shift in the free layer R-H loop was found. Since the two samples were patterned from the same wafer, the shift (offset field) values are similar (∼57 Oe for Sample A, and ∼60 Oe for Sample B). An external field was applied during the STT switching probability measurement in order to cancel the offset field. The TMR ratio and coercivity dependence on temperature are shown in Fig. 1(c) and (d), respectively. The mean and standard deviation are calculated from ten measured R-H loops at each temperature point. The TMR ratio decreases by 10% (Sample A) and 14% (Sample B) from RT to 80 °C. The main reduction is in

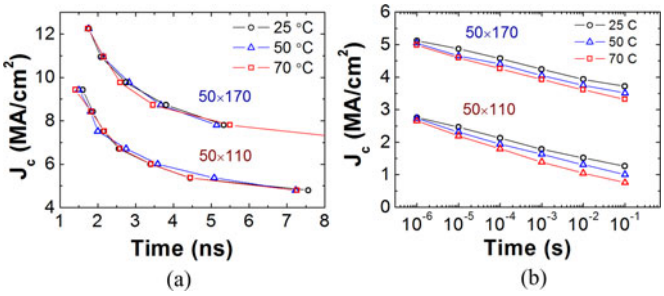

Fig. 2. (a) and (b) Switching current density at 50% switching probability versus pulse widths at short time scale (1–8 ns) and long time scale (1 μs–0.1 s).

the antiparallel state resistance, while the resistance of parallel state remains almost constant. In Fig. 1(d), we can see that for Sample A, coercivity decreases from 123 Oe to 93 Oe (24.3%); and for Sample B, it decreases from 53 Oe to 31 Oe (41.5%). The smaller thermal stability of Sample B results in higher relative coercivity reduction. Thermal stability factors are estimated to be 72 for Sample A and 29 for Sample B at RT according to the fitting in Fig. 1(d) by [Victora 1989]

$$H_C = H_K \left[1 - \left(\frac{k_B T}{K_U V} \ln \left(\frac{\tau}{\tau_0} \right) \right)^{2/3} \right]. \quad (1)$$

We further examine the temperature dependence of STT switching for those MTJ samples. Fig. 2(a) and (b) shows the switching current density value at 50% switching probability in the short-time regime and long-time regime, respectively. It is clear that in the nanosecond time scale, the switching current densities at three temperatures overlap with each other, while in the long-time regime ($>$1 μs), there is an obvious switching current density reduction with the increase of the environmental temperature. The longer the switching time, the more the switching current decreases. Before further analysis, the Ohmic heating effect should be estimated. Since the antiparallel state resistance has a strong dependence on temperature as discussed in Fig. 1(c), it is used as a reference to determine the sample temperature during pulse onset period. We measured the antiparallel resistance under 0.8 V continuously (corresponding to J = 8 and 10 MA/cm^2 for Samples B and A) and found no detectable resistance reduction with the time for 1 s (measurement error $\pm$0.65 Ω). It means the temperature rising during this 1 s period is negligible. In the switching probability measurement as shown in Fig. 2, the pulse widths are below 0.1 s and there is enough idle time ($>$0.5 s) between each pulse for heat dissipation. Therefore, the Ohmic heating is not the main reason for the strong dependence of STT switching current on the environmental temperature in the long-pulse regime. These results could be explained by the two classic STT switching mechanisms. In the long-time regime, the free layer reversal happens by a thermally activated STT switching, so the environmental temperature has more contribution during the switching process. On the other hand, in the short-time regime, it is mainly a dynamic precessional switching process that is determined by the spin momentum transfer, relatively independent from the environmental temperature. We also

Table 1. Comparison of thermal stability factors.

Our Result			Grandis [Driskill-Smith 2010]			MagIC-IBM [Min 2010]		
Δ(I)[a]	Δ(H)[b]	Δ(H):Δ(I)	Δ(I)[a]	Δ(H)[b]	Δ(H):Δ(I)	Δ(I)[a]	Δ(H)[b]	Δ(H):Δ(I)
32	29	0.906	32	40	1.25	58.3	120	2.06
47	72	1.53	36	65	1.81	63.5	135	2.13

[a] Thermal stability factor measured by current ramping method (2).
[b] Thermal stability factor measured by magnetic characterization.

estimate the thermal stability factor at three temperatures by the data presented in Fig. 2(b) according to [Sun 2000]

$$J_c(\tau) = J_{c0}\left[1 - \frac{k_B T}{K_U V}\ln\left(\frac{\tau}{\tau_0}\right)\right]. \quad (2)$$

The fitted thermal stability factors are 47 (at 25 °C), 46 (at 50 °C), and 41 (at 70 °C) for Sample A and 32 (at 25 °C), 30 (at 50 °C), and 28 (at 70 °C) for Sample B. We notice that the fitted thermal stability factor for Sample A here is much smaller compared to the previous value (72). A similar discrepancy has been reported in several other works as summarized in Table 1. It seems that the current ramping method usually gives an underestimated thermal stability factor compared to other methods which measure the thermal stability factor from magnetic characterization. The most possible reason for this discrepancy is that STT may induce nonuniform switching. Therefore, (2) derived from the macrospin model may not be valid. This can also explain the observation that a larger discrepancy was found in more thermally stable samples according to Table 1, since higher thermal stability may come from larger sample sizes or aspect ratios (as in our study here) and, thus, lead to a more serious nonuniform magnetization distribution.

We show the measured STT switching probability cdf curves of Sample A at 100 ms, 10 μs, and 10 ns under three temperatures in Fig. 3(a).The derivative of CDF curve is called probability density function (pdf) as plotted in Fig. 3(b). It is notable that not only the median point of the switching current density reduces with the increase of temperature as mentioned previously, but also the whole switching pdf shifts together to the left when the sample is heated. This shift is more obvious for long pulses. The width of the switching pdf remains almost constant at all temperatures. The switching pdfs are fitted by (3) [Li 2004, Koch 2004]. These fitted results are indicated by the solid curve in Fig. 3(b). Although (3) was deduced from the thermal activation model, the shape of the switching pdf still agrees very well with it in all time scales. However, in order to describe the increase of the distribution width with the decrease of the pulse width, the fitted thermal stability values have to be 46, 31, and 14 for 100 ms, 10 μs, and 10 ns respectively. This may imply that modifications are possibly required for (3) when using it to carry out the design margin estimation for STT-RAM application [Chen 2010, Takemura 2008]

$$p\left(\frac{J}{J_{c0}}\right) = \Delta\frac{\tau}{\tau_0 \exp\left(\Delta\left(1 - J/J_{c0}\right)\right)} \cdot \exp\left(\frac{-\tau}{\tau_0 \exp\left(\Delta\left(1 - J/J_{c0}\right)\right)}\right), \quad \Delta = \frac{K_U V}{k_B T}. \quad (3)$$

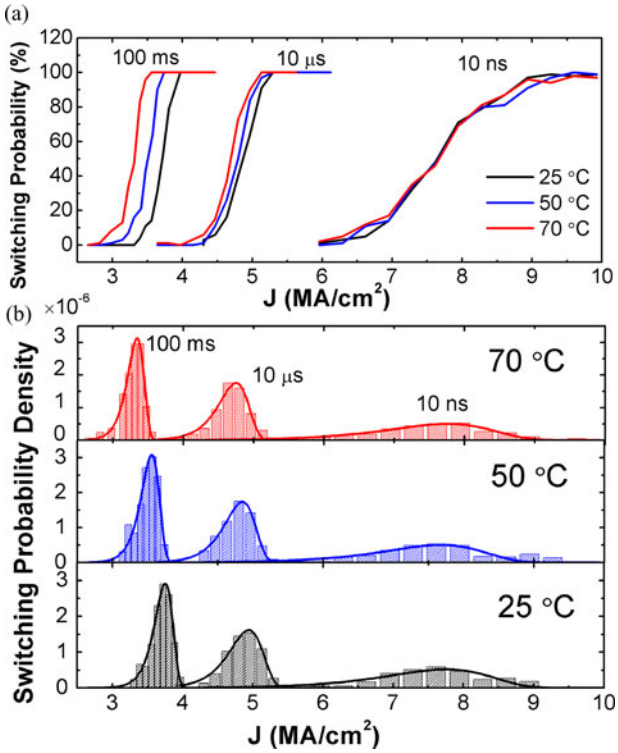

Fig. 3. (a) Switching probability as a function of current density measured in Sample A at 100 ms, 10 μs, and 10 ns. (b) Switching probability density of sample A. The bars are experimental data and solid curves are fitted data.

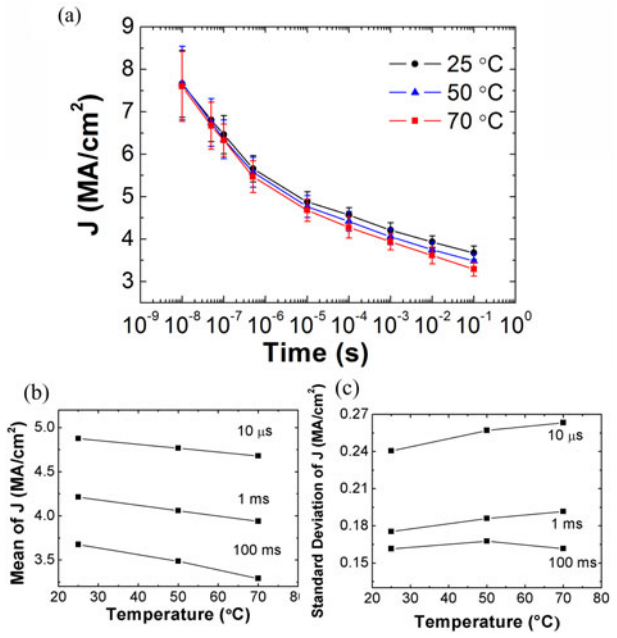

Fig. 4. (a) Current density from 10 ns to 0.1 s measured in Sample A. Each symbol represents the mean value and error bars indicate the standard deviation. (b) and (c) Mean and standard deviation of switching current density as a function of temperature measured in Sample A.

The mean and standard deviation (1σ) of Sample A from 10 ns to 0.1 s are summarized in Fig. 4(a). Similar to the result by Wang et al. [2009] and Driskill-Smith et al. [2010], the

standard deviation increases dramatically with the decrease of pulse width especially below 1 μs. A simple explanation is that the variation from thermal fluctuation gets more chance to be averaged out in a longer time. A complete picture of switching current variation versus time was given by solving the stochastic Landau–Lifshitz–Gilbert equation numerically [Wang 2009]. In Fig. 4(b) and (c), we also notice that the decreased energy barrier by the environmental temperature has more impact on the median point rather than the variation of switching current. This may be because in the particular temperature range (25–70 °C) that we are interested, the decrease in the thermal stability is too small (from 47 to 41) to have a large influence on the switching current variation. As a result, the pulse width is the more important factor to be concerned with compared to the working temperature regarding the switching current variation in STT-RAM design.

IV. CONCLUSION

We have investigated the MTJ memory cell performance in a temperature range close to the possible working environment for the STT-RAM application (25 °C–80 °C). The temperature dependences of TMR ratio, coercivity, thermal stability factor, and STT switching current density distribution were studied. One important observation was that, due to two distinct STT switching mechanisms, the influence of the environmental temperature on the switching current greatly depended on the switching time. As the temperature increases, the switching current density reduction with temperature was only found in the long pulse range ($>$1 μs), not in the short pulse range ($<$10 ns). Furthermore, in the particular temperature range that we are interested, the switching current density variation was found to be less sensitive to the environmental temperature compared to the switching time, which means the latter is the more important factor to be considered in STT-RAM design.

ACKNOWLEDGMENT

This work was supported in part by the Defense Advanced Research Projects Academy Spin Torque Transfer-Random Access Memory Program under Grant HR0011-09-C-0114 and the National Science Foundation Materials Research Science and Engineering Center Program, University of Minnesota, under Grant DMR-0819885. The work of H. Zhao and J.-P. Wang was supported by an Intel University Research Grant.

REFERENCES

Berger L (1996), "Emission of spin waves by a magnetic multilayer traversed by a current," *Phys. Rev. B*, vol. 54, pp. 9353–9358, doi: 10.1103/PhysRevB.54.9353.

Chen E, Apalkov D, Diao Z, Driskill-Smith A, Druist D, Lottis D, Nikitin V, Tang X, Watts S, Wang S, Wolf S A, Ghosh A W, Lu J W, Poon S J, Stan M, Butler W H, Gupta S, Mewes C, Mewes T, Visscher P B (2010), "Advances and future prospects of spin-transfer torque random access memory," *IEEE Trans. Magn.*, vol. 46, pp. 1873–1878, doi: 10.1109/TMAG.2010.2042041.

Driskill-Smith A, Watts S, Nikitin V, Apalkov D, Druist D, Kawakami R, Tang X, Luo X, Ong A, Chen E (2010), "Non-volatile spin-transfer torque RAM (STT-RAM): Data, analysis and design requirement for thermal stability," in *Proc. Symp. VLSI Technol.*, pp. 51–52, doi: 10.1109/VLSIT.2010.5556124.

Heindl R, Rippard W H, Russek S E, Kos A B (2011), "Physical limitations to efficient high-speed spin-torque switching in magnetic tunnel junctions," *Phys. Rev. B*, vol. 83, 054430, doi: 10.1103/PhysRevB.83.054430.

Higo Y (2005), "Thermal activation effect on spin transfer switching in magnetic tunnel junctions," *Appl. Phys. Lett.*, vol. 87, 082502, doi: 10.1063/1.2011795.

Katine J A, Fullerton E E (2008), "Device implications of spin-transfer torques," *J. Magn. Magn. Mater.*, vol. 320, pp. 1217–1226, doi: 10.1016/j.jmmm.2007.12.013.

Kawahara T (2011), "Challenges toward gigabit-scale spin-transfer torque random access memory and beyond for normally off, green information technology infrastructure (Invited)," *J. Appl. Phys.*, vol. 109, 07D325, doi: 10.1063/1.3556681.

Koch R H, Katine J A, Sun J Z (2004), "Time-resolved reversal of spin-transfer switching in a nanomagnet," *Phys. Rev. Lett.*, vol. 92, 088302, doi: 10.1103/PhysRevLett.92.088302.

Krivorotov I N, Emley N C, Garcia A G F, Sankey J C, Kiselev S I, Ralph D C, Buhrman R A (2004), "Temperature dependence of spin-transfer-induced switching of nanomagnets," *Phys. Rev. Lett.*, vol. 93, 166603, doi: 10.1103/PhysRevLett.93.166603.

Li Z, Zhang S (2004), "Thermally assisted magnetization reversal in the presence of a spin-transfer torque," *Phys. Rev. B*, vol. 69, 134416, doi: 10.1103/PhysRevB.69.134416.

Meng H, Wang J P (2006), "Composite free layer for high density magnetic random access memory with lower spin transfer current," *Appl. Phys. Lett.*, vol. 89, 152509, doi: 10.1063/1.2361280.

Min T, Chen Q, Beach R, Jan G, Horng C, Kula W, Torng T, Tong R, Zhong T, Tang D, Wang P, Chen M-M, Sun J Z, Debrosse J K, Worledge D C, Maffitt T M, Gallagher W J (2010), "A study of write margin of spin torque transfer magnetic random access memory technology," *IEEE Trans. Magn.*, vol. 46, pp. 2322–2327, doi: 10.1109/TMAG.2010.2043069.

Myers E B, Albert F J, Sankey J C, Bonet E, Buhrman R A, Ralph D C (2002), "Thermally activated magnetic reversal induced by a spin-polarized current," *Phys. Rev. Lett.*, vol. 89, 196801, doi: 10.1103/PhysRevLett.89.196801.

Seki T (2011), "Switching-probability distribution of spin-torque switching in MgO-based magnetic tunnel junctions," *Appl. Phys. Lett.*, vol. 99, 112504, doi: 10.1063/1.3637545.

Slonczewski J C (1996), "Current-driven excitation of magnetic multilayers," *J. Magn. Magn. Mater.*, vol. 159, pp. L1–L7, doi: 10.1016/0304-8853(96)00062-5.

Sun J Z (2000), "Spin-current interaction with a monodomain magnetic body: A model study," *Phys. Rev. B*, vol. 62, pp. 570–578, doi: 10.1103/PhysRevB.62.570.

Takemura R, Kawahara T, Hayakawa J, Miura K, Ito K, Yamanouchi M, Ikeda S, Takahashi H, Matsuoka H, Ohno H (2008), "TMR design methodology for spin-transfer torque RAM (SPRAM) with nonvolatile and SRAM compatible operations," in *Proc. Non-Volatile Semicond. Memory Workshop, Int. Conf. Memory Technol. Design*, Opio, France, 2008, pp. 54–56, doi: 10.1109/NVSMW.2008.22.

Victora R H (1989), "Predicted time dependence of the switching field for magnetic materials," *Phys. Rev. Lett.*, vol. 63, pp. 457–460, doi: 10.1103/PhysRevLett.63.457.

Wang X, Zhu W, Siegert M, Dimitrov D (2009), "Spin torque induced magnetization switching variations," *IEEE Trans. Magn.*, vol. 45, pp. 2038–2041, doi: 10.1109/TMAG.2009.2015376 .

Zhao H, Lyle A, Zhang Y, Amiri K P, Rowlands G, Zeng Z et al. (2011), "Low writing energy and sub nano-second spin torque transfer switching of in-plane magnetic tunnel junction for STT-RAM," *J. Appl. Phys.*, vol. 109, p. 07C720, doi: 10.1063/1.3556784.